Remote Sensing in Ecology and Conservation
Open Access
ZSL

RESEARCH ARTICLE

Deep learning-based training data augmentation combined with post-classification improves the classification accuracy for dominant and scattered invasive forest tree species

Szilárd Balázs Likó[1], Imre J. Holb[2,3], Viktor Oláh[4], Péter Burai[5] & Szilárd Szabó[6]

[1]Department of Physical Geography, Faculty of Science, Institute of Geography and Earth Sciences, Eötvös Loránd University, Pázmány Péter sétány 1/A, Budapest 1117, Hungary
[2]Institute of Horticulture, Faculty of Agricultural and Food Sciences and Environmental Management, University of Debrecen, Böszörményi út 138, Debrecen H-4032, Hungary
[3]Plant Protection Institute, Centre for Agricultural Research, Eötvös Loránd Research Network (ELKH), Herman Ottó út 15, Budapest 1022, Hungary
[4]Department of Botany, Faculty of Science and Technology, University of Debrecen, Egyetem tér 1, Debrecen H-4032, Hungary
[5]Remote Sensing Centre, University of Debrecen, Böszörményi út 138, Debrecen H-4032, Hungary
[6]Department of Physical Geography and Geoinformatics, Faculty of Science and Technology, University of Debrecen, Egyetem tér 1, Debrecen 4032, Hungary

Keywords
Ailanthus, black locust, Convolutional Neural Network, multiresolution segmentation, Random Forest, Support Vector Machine

Correspondence
Imre J. Holb, Institute of Horticulture, Faculty of Agricultural and Food Sciences and Environmental Management, University of Debrecen, Böszörményi út 138, 4032 Debrecen, Hungary. Tel: +3652508444;
E-mail: holbimre@gmail.com

Funding Information
The research was supported by the professional support of the Doctoral Student Scholarship Program of the Co-operative Doctoral Program of the Ministry of Innovation and Technology, the K138079, K138503, K131478 and the KKP144068 Nemzeti Kutatási Fejlesztési Hivatal projects.

Editor: Temuulen Sankey
Associate Editor: Bin Chen

Received: 14 March 2023; Revised: 25 June 2023; Accepted: 12 July 2023

doi: 10.1002/rse2.365

Abstract

Species composition of forests is a very important component from the point of view of nature conservation and forestry. We aimed to identify 10 tree species in a hilly forest stand using a hyperspectral aerial image with a particular focus on two invasive species, namely Ailanthus tree and black locust. Deep learning-based training data augmentation (TDA) and post-classification techniques were tested with Random Forest and Support Vector Machine (SVM) classifiers. SVM had better performance with 81.6% overall accuracy (OA). TDA increased the OA to 82.5% and post-classification with segmentation improved the total accuracy to 86.2%. The class-level performance was more convincing: the invasive Ailanthus trees were identified with 40% higher producer's and user's accuracies (PA and UA) to 70% related to the common technique (using a training dataset and classifying the trees). The PA and UA did not change in the case of the other invasive species, black locust. Accordingly, this new method identifies well Ailanthus, a sparsely distributed species in the area; while it was less efficient with black locust that dominates larger patches in the stand. The combination of the two ancillary steps of hyperspectral image classification proved to be reasonable and can support forest management planning and nature conservation in the future.

Introduction

Composition and spatial distribution of species is one of the basic features defining the structure and functioning of forest stands. Gathering stand-level data, therefore, is important for implementing sustainable forest management practices in order to preserve biodiversity and multifunctional ecosystem services (Vo et al., 2013). Knowledge on the species composition is also important in quantifying timber volume and above ground biomass (Brahma et al., 2021; Nagy et al., 2020; Vo et al., 2013; Vorster et al., 2020), in nature conservation and landscape protection (Blackman, 2013; Zhang & Xie, 2012), and in tracking the spread of invasive tree species (Asner et al., 2008; Wilfong et al., 2009; Baron et al., 2018; Dyderski & Jagodziński, 2020; Dyderski & Pawlik, 2020; Dyrmann et al., 2021; Lake et al., 2022; da Silva et al., 2023).

Among invasive trees, black locust (*Robinia pseudoacacia* L.) is a species of particular concern. It is native in North America and is used for afforestation in many European, African and Asian countries. *R. pseudoacacia* is a nitrogen-fixing leguminous tree, well adapted to extreme conditions such as drought, nutrient-poor soils, pollution and high light. It can spread quickly as a thorny pioneer tree in disturbed habitats, including recently coppiced stands, forest edges and urbanized landscapes (Hanover & Mebrahtu, 1991). In addition, it is highly resilient after establishing a population and has the ability to propagate vegetatively via runners, resprout after cutting and preserve seed viability in the soil for years (Cierjacks et al., 2013). Another dangerous species is Ailanthus tree [*Ailanthus altissima* (Mill.) Swingle], considered as invasive in the USA and Europe, especially in the Mediterranean regions, due to its high growth and reproduction rates, and efficient dispersal (Cronk & Fuller, 1995; Feret, 1985; Landenberger et al., 2009; Nava, 2014; Shah, 1997). Similarly to black locust, Ailanthus trees are highly tolerant to drought and air pollution (Feret, 1985; Shah, 1997). In addition to their resilience and spreading potential, both species have been reported to be strongly allelopathic (Heisey, 1990; Nasir et al., 2005). Thus, by rapidly colonizing new patches and suppressing understorey herbs and tree saplings, these species pose a threat to forests by decreasing biodiversity and tree recruitment (Radtke et al., 2013).

Mapping invasive plants or trees can be the first step in fighting these unwanted species. Ground-based tree species mapping is, however, challenging and requires experts working in the field, Global Navigation Satellite Systems devices to ensure high accuracy positioning and time. It is difficult to find every individual in the field, especially those of the ecologically detrimental Ailanthus trees. These trees can grow high and their crowns merge into the canopy, or even emerges above it, thus blocking the light from the surrounding endemic trees (Feret, 1985; Nava, 2014; Shah, 1997). Timely identification of the scattered Ailanthus trees in forest stands is, however, crucial because this species can occupy considerable areas every year after its first appearance. Due to this tree's special characteristics, aerial identification seems to be a promising solution, and there are examples of mapping from helicopter with a 'spotter' and a 'sketchmapper' (Rebbeck et al., 2015). Aerial imaging with multispectral or hyperspectral cameras, or satellite images, on the other hand, may offer even higher efficiency. Examples of a successful application of multispectral imaging in species-level mapping have already been reported (Ke et al., 2010). In the present study, however, we focused on hyperspectral survey.

Hyperspectral sensors can be mounted on different platforms: uncrewed aerial systems (UASs), aircraft and satellites. UASs solutions are suitable for smaller areas (1–50 ha), while in larger areas aircraft or satellite systems are more appropriate (Borengasser et al., 2007; Pu, 2017; Zhang et al., 2020). The limitations are also different for each platform: UASs can be limited by wind and rain, while aircraft can fly in a wider range of weather conditions, but cloudy circumstances may bias the collected data. Similarly, satellite data is also limited by clouds (Borengasser et al., 2007; Casagrande, 2018; Pu, 2017). Spatial resolution (ground sampling distance, GSD) can also be an important factor when choosing the most suitable platform: UASs' hyperspectral sensors usually have a GSD of 0.1–0.5 m depending on the flight height, while in case of aircraft GSD can be 1–2 m. Currently, only a few hyperspectral satellite data sources are publicly available: the PRISMA (Vangi et al., 2021), the EnMap (Guanter et al., 2015; Stuffler et al., 2007) and the DESIS (Farmonov et al., 2023; Müller et al., 2016); all three systems featuring 30 m GSD. For tree species mapping, the appropriate pixel size is 1 m (e.g., Brovkina et al., 2015; Burai et al., 2019; Likó et al., 2022; Merentitis et al., 2014), thus favoring UASs- and aircraft-based data gathering in such applications.

Among the wide palette of image processing algorithms, deep learning (DL) is a rapidly spreading technique. Due to its effectiveness, it is expected to gain increasing popularity in the near future, along with improving technology and computing capacity on the processing side (Ma et al., 2019). Compared to traditional machine learning, DL can improve its own predictions without external help and data processes. DLs have several approaches, and beside the original algorithms there are numerous improvements, too. Convolutional Neural Network (CNN) is effective in extracting complex and

essential features from raw or unprocessed images with examining the images in smaller and smaller windows (Zhu et al., 2017), which is efficient in case of hyperspectral data. A further strength of CNN is that it is widely accessible, has been implemented in several software and is relatively easy to use. However, the large training datasets required by DLs (including CNN) can limit their application when data collection involves extensive fieldwork.

Extending the training dataset is a commonly used method to improve the efficiency of classification. There are several possible approaches to augment the existing limited data with transformations, such as rotation and scaling when using ground truth images, or unsupervised pre-training with ground truth pixels (Hinton et al., 2006; Zhao & Du, 2016). However, in highly diverse woodlands, generalizations on choosing one best method are hard to make due to the species complexity.

Different methods have been developed in order to improve accuracy, such as using textural information, spectral indices, ancillary data, visual interpretation, smoothing or post-classification (e.g., Bhosale et al., 2014; El-Hattab, 2016; Likó et al., 2022; Manandhar et al., 2009; Thakkar et al., 2017), but there is no standard methodology to choose one. The selection or development of the most effective procedure is highly dependent on multiple factors i.e., the target object (plant), the initial dataset and the obtained results before performing the post-classification procedure. Data augmentation can be performed by local spectral variance analysis that examines the spectral attributions of the original training dataset and then expands it within the variance level (Lv et al., 2020; Shorten & Khoshgoftaar, 2019). Another type of augmentation is the hierarchical random sampling (Zhang & Shao, 2021). DL-based methods had also appeared in the recent years, such as semi-supervised stacked autoencoders with co-training (Zhou et al., 2019). Furthermore, in the last 10–15 years, object-based classifications have proven to be effective too (Aguirre-Gutiérrez et al., 2012). The main advantage of object-based methods is their applicability in combining multiple images with even different spatial resolution on segment level in order to feed additional information (Amini et al., 2018). Generally, hyperspectral images can ensure appropriate input data for tree species mapping, but high-resolution satellite images can perform even better. Thus, image processing itself is still challenging, and any small developments or additional steps can help to achieve higher accuracy, i.e., to identify invasive or valuable trees. Therefore, we focused on two possible approaches which can provide us higher efficiency compared to the traditional image classification (i.e., training–predicting–testing).

The overall aim of this study was to improve thematic accuracy for mapping two invasive tree species by using hyperspectral imagery, namely *A. altissima* that shows rather scattered distribution, and *R. pseudoacacia* that dominates larger patches. We focused on two different areas where classification accuracies could be improved: (i) a DL-based method was used to increase the training dataset as a pre-classification data treatment, and (ii) a stepwise region-growing segmentation was applied to filter single pixels as a post-classification method.

Materials and Methods

Study area

The study area (170 ha) was located near (3–4 km) to Pécs city (South Hungary, 46°08′06.90″ N, 18°15′55.60″ E), in a hilly area with the average height of ~320 m above sea level (Fig. 1). The area is part of the Mecsek Park Forest, predominantly composed of native species but, more recently, the spreading invasive trees pose an increasing threat. The study area consists of various woodland types. The vegetation cover of the wider area is also very diverse, containing both sub-Mediterranean, Balkanic and sub-Atlantic species, combined with sub-Mediterranean loess grasslands. The climate is warm and moderately humid on the southern slopes, and the annual precipitation is ~700 mm. The dominant soil type is highly acidic Luvisol (Kevey & Borhidi, 2005). The species distribution and vegetation dynamics are typical in Central European level; thus, it can serve as an example for other studies, too. Furthermore, the presence of two invasive trees, black locust and

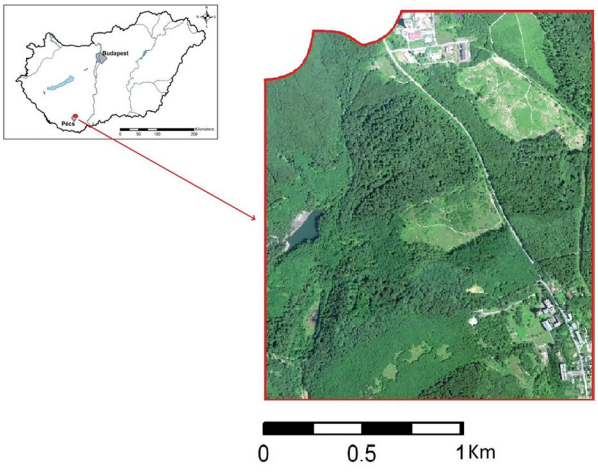

Figure 1. Location of the study area, near Pécs city, Hungary.

Ailanthus, was important, too, as focal species of our investigations.

Hyperspectral data

The hyperspectral imaging survey was conducted on 29 June, 2016 with an Asia KESTREL 10 sensor (Aeroscout, Horw, Switzerland) placed on a piloted aircraft, with a spectral range of 375–2500 nm in 420 spectral bands and with a GSD of 1 m. Geometric and radiometric corrections had been performed with CaliGeoPRO software (SPECIM, Spectral Imaging, Ltd., West Allis, WI, USA). The noisy bands with high noise-to-signal ratio were removed based on visual inspection. The survey covered a smaller area; thus, an empirical line model was applied to provide atmospheric correction, which is an effective alternative to radiative transfer modeling approaches (Karpouzli & Malthus, 2003). Artificial objects were masked *via* manual delineation as well as areas with <3 m above ground height as computed from LiDAR data.

Reference dataset

Ten tree species were selected based on field observations and visual analysis of the aerial image (Table 1), with a special focus on *R. pseudoacacia* and *A. altissima*.

The selected species were dominant in the canopy of the ground observation spots, except *A. altissima*, that had rather scattered spatial distribution. A total of 4811 pixels were recorded as reference data with polygons covering the canopy of the identified individuals. Next, by using the polygons, we randomly split the data into training and testing datasets in 60:40 ratio. We applied the Jeffries–Matusita distance to investigate the statistical separability of spectra of classes (Wang et al., 2019).

Table 1. Scientific name, common name, abbreviation, numbers of training and testing pixels of 10 tree species assessed in the study area (Pécs, Hungary, 2016).

Scientific name	Common name	Abbreviation	Training pixels	Testing pixels
Robinia pseudoacacia L.	Black locust	BL	1197	600
Fagus sylvatica L.	Common beech	CB	153	67
Ailanthus altissima (Mill.) Swingle	Ailanthus	A	717	38
Cerasus avium (L.) Moench	Sweet cherry	SC	245	65
Tilia tomentosa Moench	Silver linden	SL	150	66
Carpinus betulus L.	European hornbeam	EH	83	44
Acer pseudoplatanus L.	Sycamore maple	SM	94	27
Quercus robur L.	English oak	EO	270	76
Quercus petraea (Matt.) Liebl.	Sessile oak	SO	381	134
Picea abies (L.) H. Karst.	Norway spruce	NS	67	27

Image processing

The image processing workflow included four main steps: feature extraction, training data augmentation (TDA), classification with machine learning algorithms and post-classification, respectively (Fig. 2).

Feature extraction

Hyperspectral data is useful due to its almost continuous spectral profile, but the large number of bands also means redundant spectral information because of the strong correlation of consecutive bands (Zhang & Xie, 2012). Besides, the large number of bands assumes large set of training pixels in the classification phase, which decreases classification accuracy. One possible solution is the dimension reduction, which aggregates the information into fewer artificial components preserving the maximal explained variance. We chose the minimum noise fraction (MNF) transformation (Fig. 2), which is based on two consecutive principal component analyses (PCAs): first PCA rotation aims to remove the noise bands, and the second PCA rotation is performed on the image when the first step rescaled by the noise standard deviation. The output is also similar to the PCA, the largest explained variances belong to the first 5–10 principal components (PCs) and then the contribution of the PCs' is decreasing. MNF was applied successfully as input data in several previous studies (Burai et al., 2019; Hamada et al., 2007; Likó et al., 2022; Zhang & Xie, 2012).

Training data augmentation

As the first step, a pre-classification was performed with the CNN aiming to enlarge the training dataset to help classification efficacy. Since the input requirements for CNN would have exceeded the available training dataset, we did not involve this method directly to the workflow. Instead, we augmented the original dataset by applying another option of CNN, that is, by determining probability layers (class activation raster) for each class bound to the classification result. This way, we identified pixels that may be added to the training datasets. The 10 tree species resulted in 10 activation raster layers, and we filtered the highest probabilities (from 99 to 90% by 1% steps) in

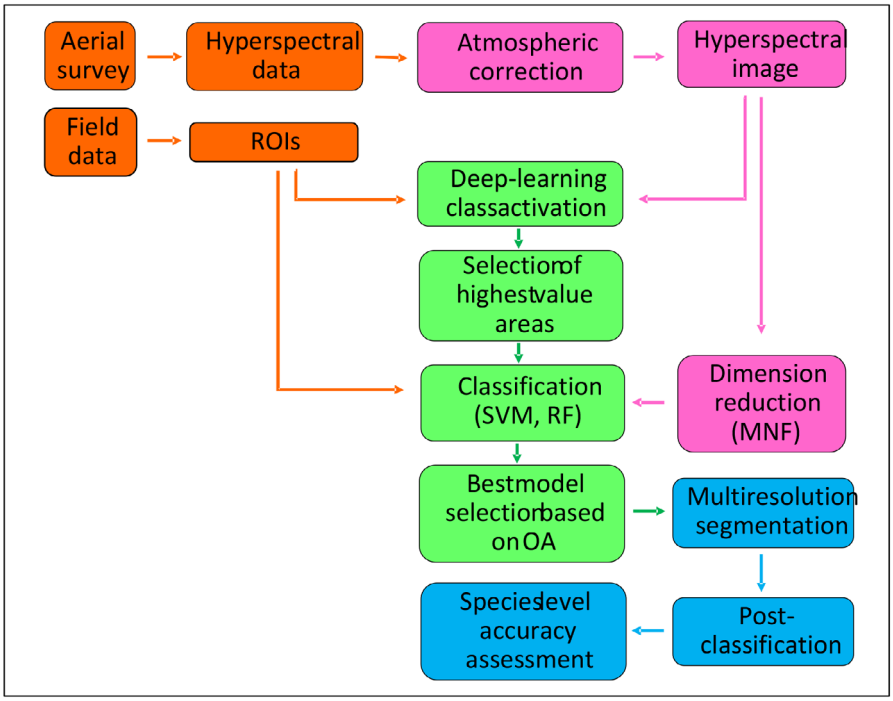

Figure 2. Workflow of image processing including feature extraction, deep learning class activation, classification with machine learning algorithms and post-classification, respectively. MNF, minimum noise fraction; OA, Overall Accuracy; RF, Random Forest; ROIs, training pixels by regions of interest; SVM, Support Vector Machine (orange boxes: input data, pink boxes: processing, green boxes: classification, blue boxes: post-classification).

each and then added these pixels to the training data. Such DL-based TDA, based on a CNN was implemented in the TensorFlow model of the ENVI 5.5 (Abadi et al., 2016; Lampe et al., 2021).

Classification algorithms

Principle components of the MNF (MCs) were the predictor variables, and two classification algorithms were applied in the analysis, the Support Vector Machine (SVM) and the Random Forest (RF), respectively (Fig. 2). Both methods are robust, have no assumptions on the training data, can operate with fewer training data and usually outperforms other methods.

The SVM uses a multidimensional hyperplane to classify the pixels of an image into predefined classes (Cortes & Vapnik, 1995; Murty & Raghava, 2016). Since hyperplane is linear, the non-linear boundaries may cause difficulties in the classification. Therefore, the SVM model uses the 'kernel-trick' to overcome this issue (Melgani & Bruzzone, 2004; Murty & Raghava, 2016), and accordingly, we used the radial basis function (RBF). Hyperparameters, the gamma for RBF kernel and the C (penalty parameter) were determined by grid search with 0.05–0.5 gamma (based on the inverse of the number of involved bands), and C was tested on a logarithmic scale from 0.001 to 1000 (0.001, 0.01. 0.1, 1, 10, 100 and 1000).

RF is a non-parametric classification algorithm built on binary decision trees; each tree is built on a random part of the data derived from the reference dataset with bootstrapping. 36.7% of the training data is kept for validation to quantify the out-of-bag error and overall accuracy (OA) (Belgiu & Dragut, 2016; Breiman, 1984, 2001; Richter et al., 2016; Szabó et al., 2021). The number of decision trees and the node size can vary, we applied 100 decision trees, and the node size was set to the square root of the number of variables (according to Hastie et al., 2009).

Each classification had been run with the 5–15 components of MCs in order to test and find the thematically most accurate results of tree species map. The classifications were conducted in Exelis Envi 5.5 (Lampe et al.,2021) and QGIS 3.6 with EnMAP-Box 3 extension (EnMAP-Box Developers, 2019).

Post-classification segmentation

Object-based image analysis (OBIA) became a successful alternative to pixel-based solutions for vegetation

mapping (Zhao et al., 2020). Segmentation divides the images into small and homogenous regions according to the given criteria and frame in one or more dimensions of features (Aksoy & Akcay, 2005). Multiresolution segmentation (MRS) is one of the most successful segmentation algorithms in the past years that aggregates pixels into growing size of segments based on the given levels in an iterative process. It has three main parameters that can be set: scale, shape and compactness (Drăguţ et al., 2010). We selected the optimal shape and compactness parameters based on the preliminary tests (with the aim to find the tree crowns); thus, 0.5 compactness and 0.3 shape values were used (Likó et al., 2022).

MRS was applied on the classified image having the highest OA (Fig. 2), similarly to our previous study (Likó et al., 2022), but we applied a more sophisticated version. The scale parameter was tested with 10 and 100 different levels, in ascending order from 1 to 10 with 1 spacing (L10–L100 levels), and from 0.1 to 10 with 0.1 spacing (L01–L100 levels). Finally, we had a 10-step and a 100-step version to test. In parallel with the increasing scale parameter, the homogeneity of the resulting segments decreased by including increasingly different pixels, which we aimed to eliminate. We then reclassified the image with the majority pixel value inside each segment to filter out the outlier pixels. Post-classification was carried out on the pixel-based classified image; thus, each class got a value from 1 to 10 (i.e., the codes of the tree species).

Accuracy assessment

Forty per cent of the reference data was used for testing (section hypersepctral data, Table 1). The classifications were evaluated by means of the following indicators to determine the thematic accuracy: OA, user's accuracy (UA), producer's accuracy (PA), and the errors of commission and omission (Congalton, 1991). We also determined the F1-scores as the harmonic mean of UA and PA (Tharwat, 2021).

Results

Training data augmentation

The original number of training pixels was below 270 for the most species, except for black locust (BL) and Ailanthus (A): the two invasive species had >700 pixels. TDA successfully increased the number of training pixels, but the increase varied by tree species (Fig. 3). Three types could be distinguished based on the efficacy of training data extension: (i) 101–161% increase: EH, BL, SL, SM, A; (ii) 161–196% increase: SC, SO; and (iii) 250–394% increase: NS, EO and CB. Based on absolute pixel numbers, the increase was only 1 for EH and 30 for BL classes, while EO performed the largest increment with 526 pixels.

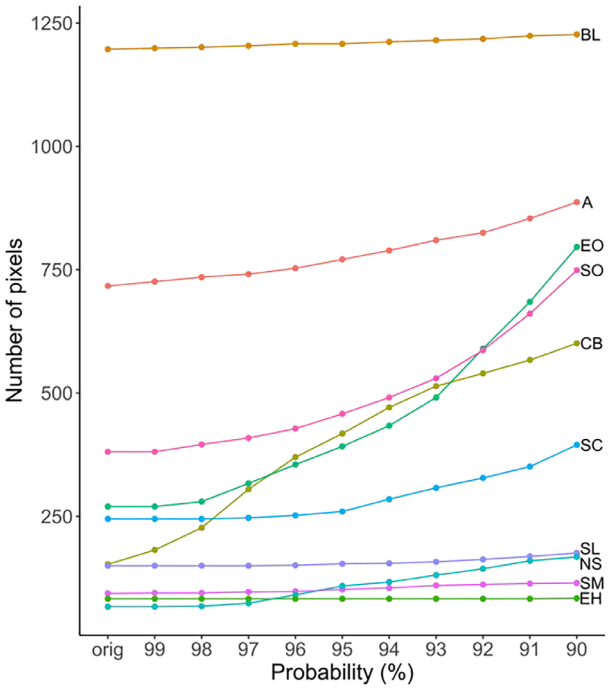

Figure 3. The increase of pixel numbers in the training dataset as a result of the CNN-based training data augmentation (orig: original training dataset, 99–90%: probability of pixels classified to a class based on the CNN-based augmentation. A, Ailanthus; BL, black locust; CB, common beech; CNN, Convolutional Neural Network; EH, European hornbeam; EO, English oak; SC, sweet cherry; SL, silver linden; SM, sycamore maple; SO, sessile oak; NS, Norway spruce.

Comparison of RF and SVM classifier

Generally, SVM provided better results than the RF: 13 MCs and the TDA pixels of 97% probability resulted in the highest OA (82.5%), which was 0.8% higher than the classification with the original training data. Using a lower probability threshold (90–94%) with the TDA resulted in lower OAs than using only the original training dataset (usually with OAs < 79%, Figs. 4 and 5).

Post-classification with segmentation

Post-classification was conducted with the most accurately classified image (SVM classifier, 13 MCs with the 97% probability pixels of TDA). Regarding the 100-level segmentation, the highest classification accuracies were obtained with the L4.9 and L5 levels, both reached 86.2% in OA, with the average object size of 62.6 and 64.8 m^2. The OA increased from L1, reached its maximum at L5

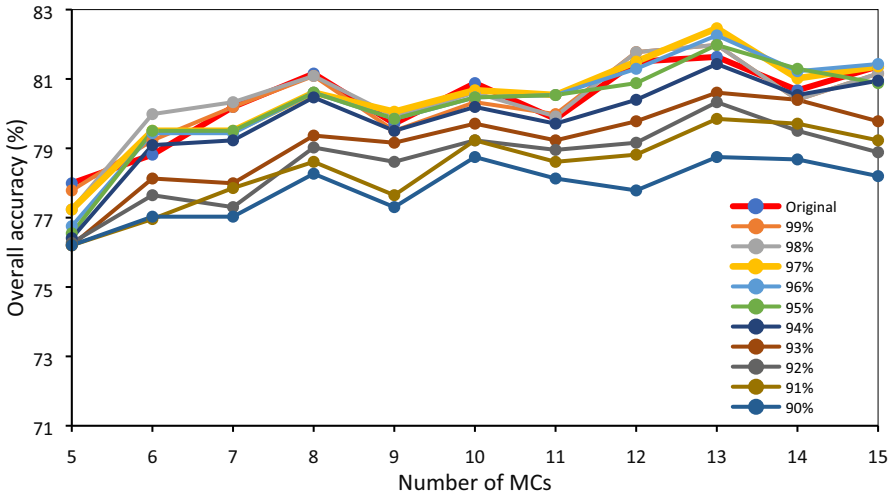

Figure 4. Overall accuracies of SVM classifications with additional pixels from the CNN-based activation layer (90–99% probability) by increasing number of MNF components (MCs). CNN, Convolutional Neural Network; MCs, principle components of the MNF; MNF, minimum noise fraction, SVM, Support Vector Machine.

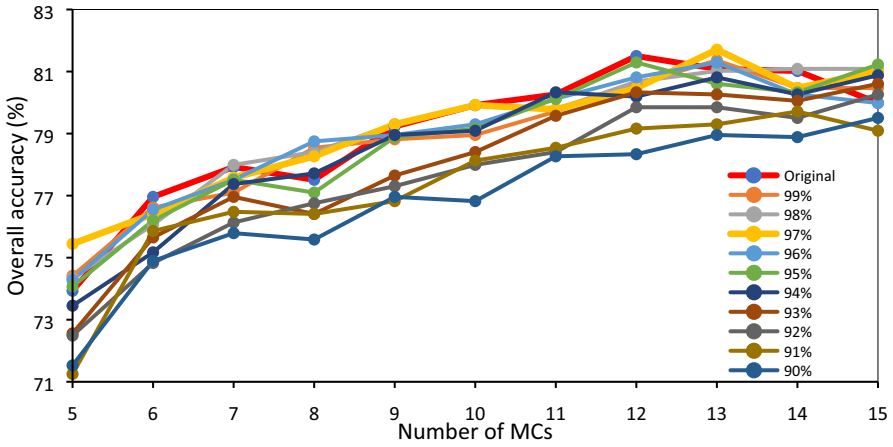

Figure 5. Overall accuracies of RF classifications with additional pixels from the CNN-based activation layer (90–99% probability) by increasing number of MNF components (MCs). CNN, Convolutional Neural Network; MCs, principle components of the MNF; MNF, minimum noise fraction; RF, Random Forest.

and then started to decrease with a spike (local maximum) at L6.2 with 85.4% and 91.2 m^2 (Fig. 6). The best result of the 10-level segmentation was achieved with the L4 level (43.6 m^2 average object size), the OA was 86.0%, that is, 3.5% better than the best model obtained with the SVM model on pixel basis. The OA raised from L1 to L4 and then began to decrease (81.2% at L5; 76.3% at L8; Fig. 6).

The 100-level segmentation yielded 0.27% higher OA compared to the 10-level approach and provided a deeper insight into the consequence of increasing the segment size. Considering the average segment areas, the differences were not relevant, and the two versions grew similarly. However, the related OAs started to show considerable differences from L5. From that point, the 10-level approach resulted in >5% worse OAs than the 100-level approach.

Class-level accuracies

F1-scores express the class-level accuracy with a single number and showed that the TDA or post-classification only slightly (<3%) improved the accuracy in case of BL, SL, and NS and had large effect in case of SC and A, while caused decreases in case of EH. The improvement in the other species were ~10% (Fig. 7).

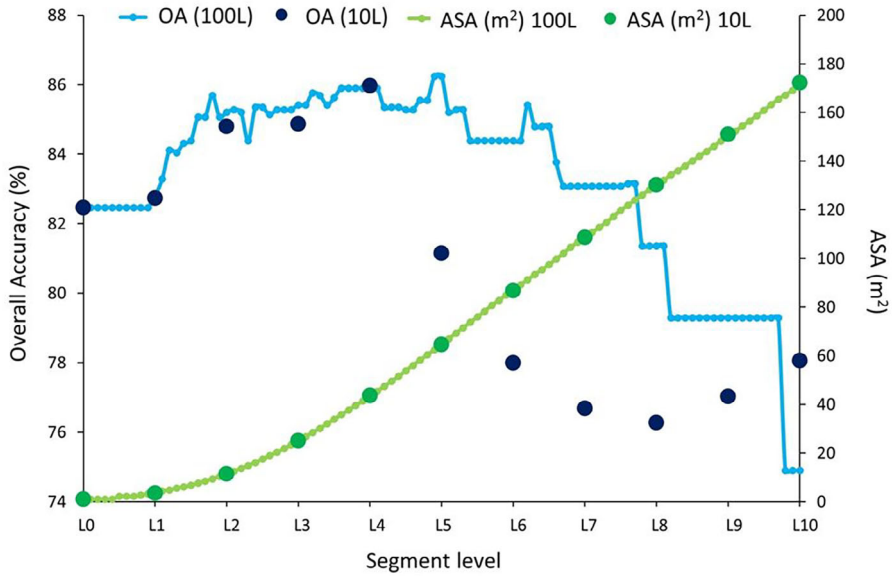

Figure 6. The effects of different segmentation levels (L0–L10) on the average segment areas (ASA), and overall accuracies (OAs) by the 10- (10L) and 100-level (100L) segmentations.

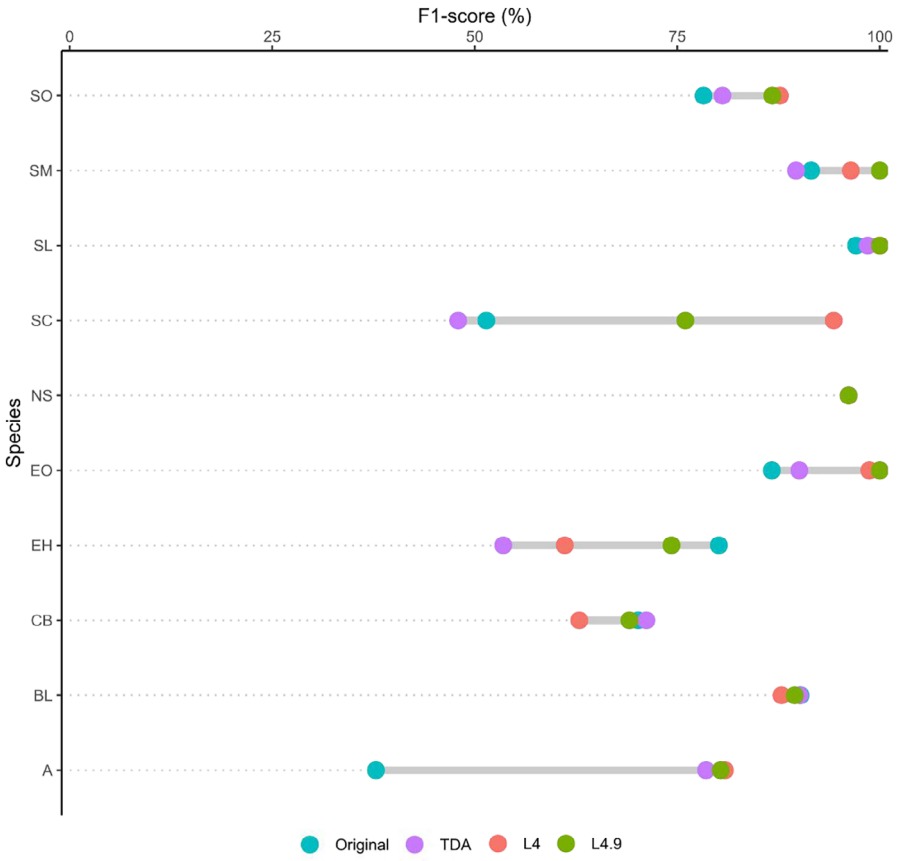

Figure 7. F1-scores of the tree species using the four approaches. A, Ailanthus; BL, black locust; CB, common beech; EH, European hornbeam; EO, English oak; NS, Norway spruce; SC, sweet cherry; SL, silver linden; SM, sycamore maple; SO, sessile oak; TDA, training data augmentation, L4 of the 10-level, and L4.9 of the 100-level versions.

We used UA and PA to observe the effects of the different approaches with more detailed insights. The result of the segmentation and the TDA approach affected the accuracy of each class in different ways (Fig. 8). There were classes with continuous improvement in both UA and PA values (EO, SL, SO and A). TDA brought the highest improvement in the case of Ailanthus, where both UA and PA values increased by ~40%. There were cases where only one accuracy metric increased while the other decreased; however, there was no clear trend (i.e., in some steps PA increased and UA decreased, but next the UA increased and the PA decreased: EH, CB, BL and SC). For the NS, there was no change in either the UA or PA. The magnitudes were considerably different; the classes of NS, EO, SM, SL and BL exceeded 80% in both PA and UA. Generally, due to the post-classification, the accuracies improved, especially in case of L4.9 level. Regarding the invasive species in our focus, the accuracy metrics of Ailanthus improved by almost 30% for both PA and UA with TDA and post-classification than could be gained with the original training dataset. Accuracies for black locust, as an opposite, did not improve. Moreover, the UA even decreased with the extension of activation pixels without the post-classification step.

The pixel-based result map contained several misclassified single pixels, even within individual tree crowns, that was almost completely fixed by the post-classification method (Fig. 9). In addition, individual tree crowns and tree clusters were also separated better.

The largest improvement was found in case of Ailanthus. TDA proved to be successful according to both the accuracy metrics and the visual inspection of maps (Fig. 10). Post-classification also ensured better results and, although the difference was slight between the L4 and L4.9 (for the 10- and 100-level segmentation approaches, respectively), the resulting map justified that selection of the applied parameters should rely on a thorough analysis. Clusters of pixels delineating actual trees instead of dispersed pixels (Fig. 10A and B) or lost information (Fig. 10C) were depicted successfully with the L4.9 (Fig. 10D).

Although the improvement in mapping black locust was not reflected by the accuracy metrics, yet it was the case for the sparsely appearing individuals (Fig. 11). In addition, the object-based post classification also helped to diminish the salt-and-pepper error of the larger stocks (Fig. 12).

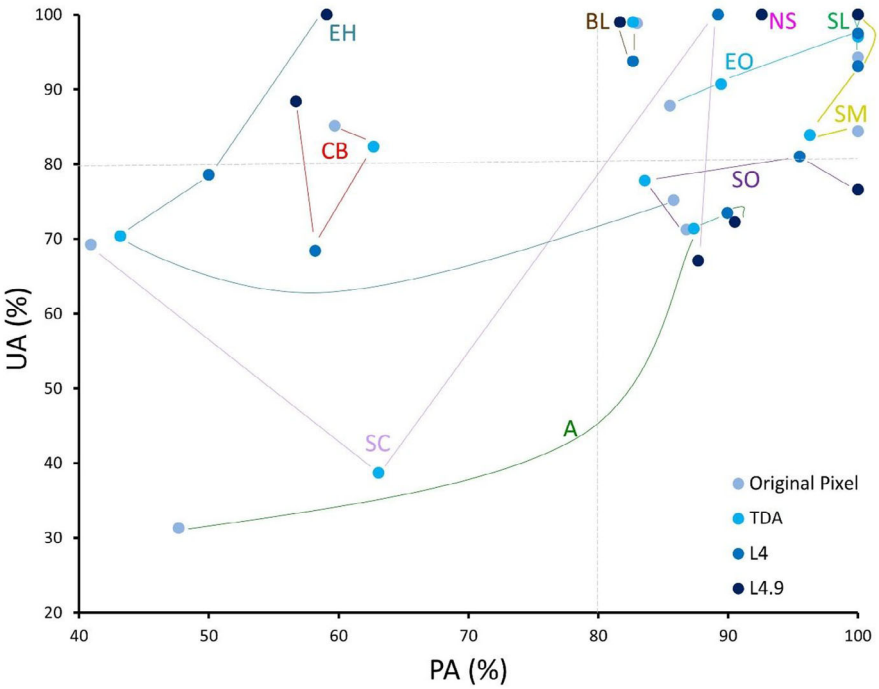

Figure 8. User's and producer's accuracies (UA and PA) of the pixel-based classification (the original with SVM and 13MCs, and the extended with 97% probability) and following the object-based reclassifications (L4 of the 10-level and L4.9 of the 100 level versions). A, Ailanthus; BL, black locust; CB, common beech; EH, European hornbeam; EO, English oak; MCs, principle components of the MNF; NS, Norway spruce; SC, sweet cherry; SL, silver linden; SM, sycamore maple; SO, sessile oak; SVM, Support Vector Machine; TDA, training data augmentation.

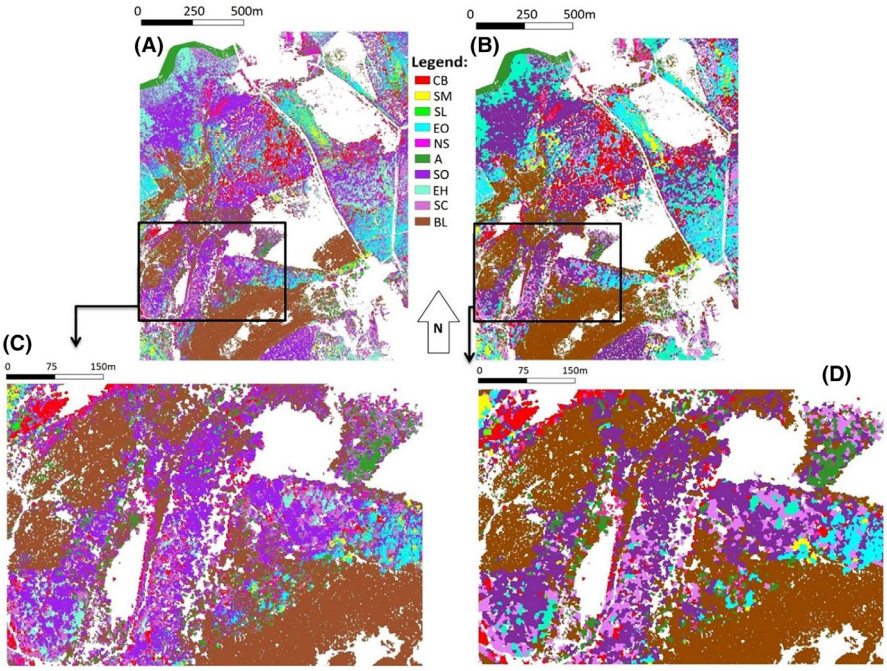

Figure 9. Species distributions according to the pixel-based classification [Support Vector Machine (SVM) classifier using 13 MCs and training data augmentation with 97% probability pixels] (A) and the object-based reclassification (reclassified at L4.9 level of segmentation) (B) of the hyperspectral image in the entire study area, as well as in a smaller sample plot (C and D, respectively). MCs, principle components of the MNF; MNF, minimum noise fraction.

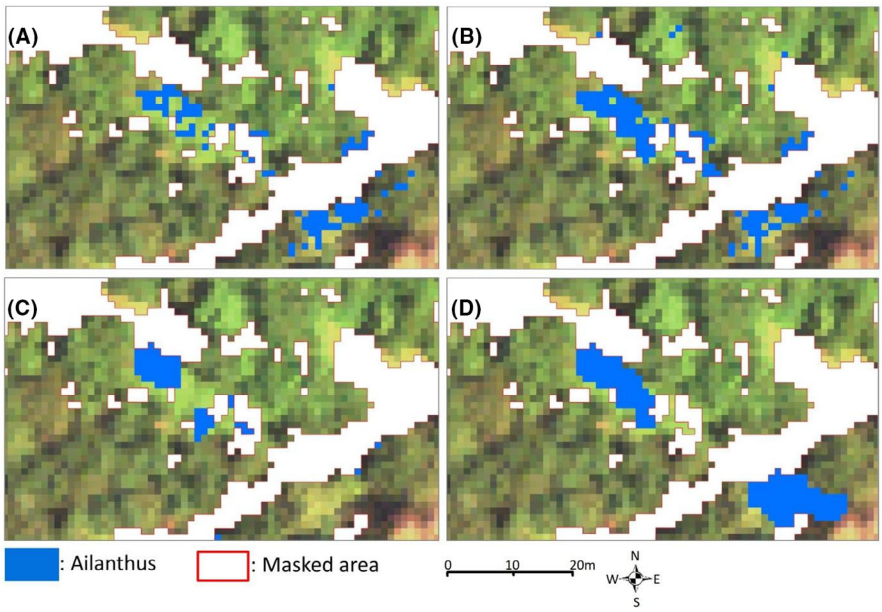

Figure 10. Maps of *Ailanthus altissima* with the original pixel-based classification (A), the pixel-based classification with extended training data (B), the object-based reclassification at L4 (C) and the object-based reclassification at L4.9 (D).

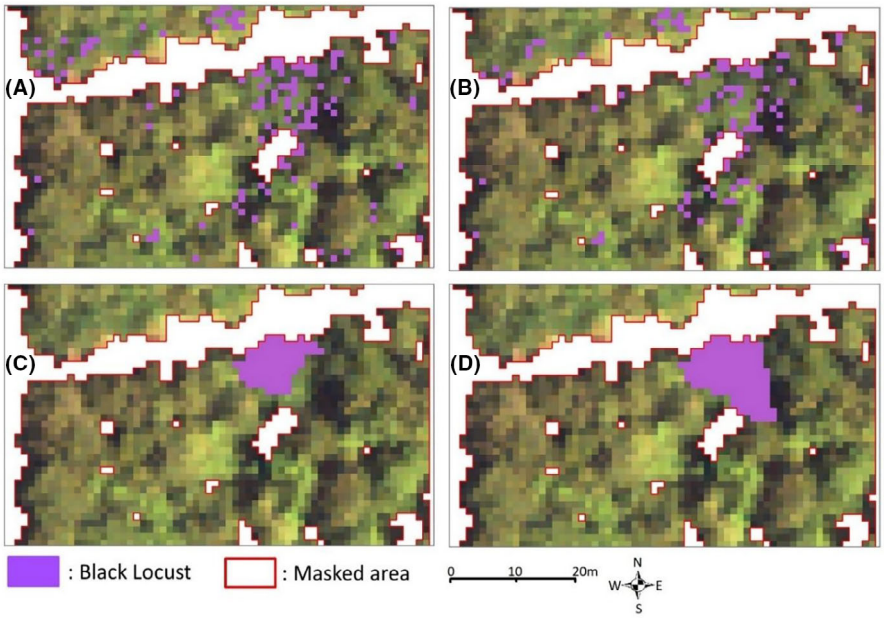

Figure 11. A section of black locust map focusing on sparsely distributed trees with the original pixel-based classification (A), the pixel-based classification with extended training data (B), the object-based reclassification at L4 (C) and the object-based reclassification at L4.9 (D).

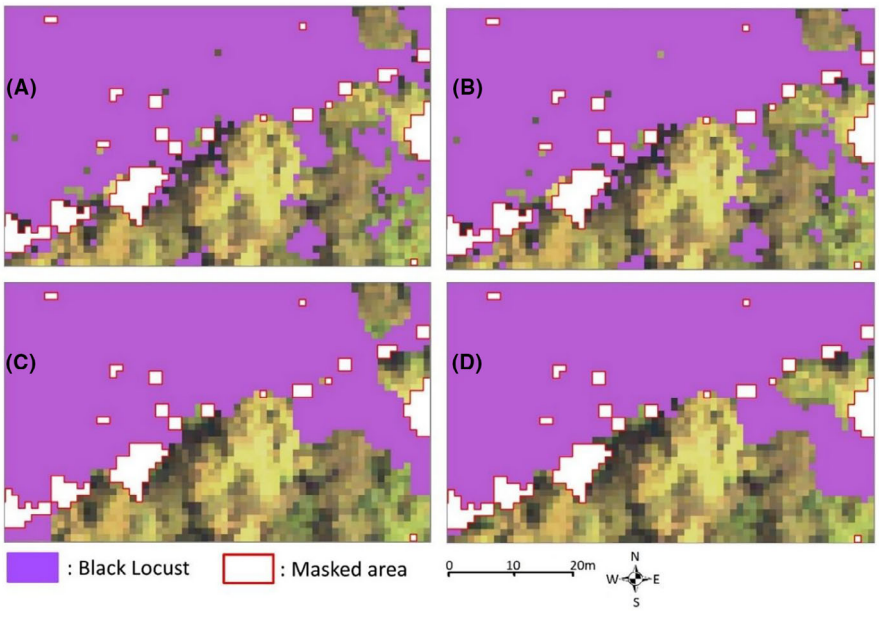

Figure 12. A section of black locust map focusing on larger stocks with the original pixel-based classification (A), the pixel-based classification with extended training data (B), the object-based reclassification at L4 (C) and the object-based reclassification at L4.9 (D).

Discussion

Invasive species pose an ever-increasing threat to the diversity and functional integrity of forested landscapes, making identification and removal of these trees one of the top priorities in forest management practice. Since ground-based observation may bottleneck efficient measures against the invaders, aerial hyperspectral images are considered to be the most promising input data for tree species mapping (Alonzo et al., 2016), even though there

are successful examples with very high-resolution satellite images too (e.g., Maurya et al., 2021; Tarantino et al., 2019). As there is no standard workflow for the image processing, all possible options should be studied and identified for better outputs. We combined two existing methods to improve the thematic accuracy and resulted in almost 5% better OA than the usual way of image processing (*i.e.*, training, model building, classification). Such an improvement was similar to those previously reported by Amini et al. (2018), Aguirre-Gutiérrez et al. (2012) and Zhang and Shao (2021). 3–5% increase may not seem to be an outstanding improvement in general terms. The increase in class-level accuracy was impressive, however, for the most concerning invasive species of the study area, that is, the Ailanthus tree. Even if our method proved to be less efficient for black locust, this latter species is considered to pose lesser threat to the communities of the area than Ailanthus.

We focused on two invasive species with different distribution patterns in the study area: black locust that forms larger homogenous patches but can also be sparsely distributed, and Ailanthus tree that is rather scattered in stands dominated by other species. Our results proved to be satisfactory for both tree species. Augmenting the training data with our TDA method helped us to gain ~40% higher UA and PA for Ailanthus, though the extension was only 24 pixels (at the applied 97% probability). It means that only a few additional – and apparently important – new data points improved the accuracy from low (30% UA) to considerably higher (70% UA), resulting in an unprecedented achievement in such distinctions. In addition, the next steps of MRS-based post-classification were also important, especially from the aspect of visualization. These steps helped to identify sparsely distributed black locust trees, which was not reflected by either UA or PA, but the visual inspection obviously proved its efficiency. Larger stands of black locust were also visualized better this way, that was supportedby the accuracy metrics. This also emphasized the fact that, beside accuracy metrics, maximizing the map product's reliability should be the final aim.

SVM's performance was slightly (<2%) better in our analyses than that of the RF's, and TDA could not ensure better OAs with RF. Contrary to this result, Shiferaw et al. (2019) reported that the RF algorithm performed the best among seven MLAs, including SVM, in generating fractional cover maps of an invasive plant species (trees of *Prosopis juliflora*) in a dryland ecosystem. This study, however, performed only comparisons of mere MLAs without any TDA and/or post-classification process. SVM and RF are both robust classification techniques, and their performance varies as a function of the number of training pixels and the number of variables. RF, as an ensemble technique with large number of decision trees, is less sensitive to the number of training data than SVM. SVM needs more training data and works well with large number of predictors (Breiman, 2001; Cortes & Vapnik, 1995). Previous studies showed that RF outperformed SVM and was more suitable for fractional cover mapping of tree species (Mi et al., 2017; Shiferaw et al., 2019). In our case, the increasing number of MCs yielded in higher OAs with RF. The same was not true for SVM: OA did not improve proportionally by increasing the number of predictors. This phenomenon was due to the fact that RF had reached ~5% lower accuracy values with the initial set of MCs.

The comparison of the results at 10 and 100L showed that the shape of the segments is as important as their size, at least for the efficiency of reclassification. Since the differences in size were negligible, differences within 1 m were typical for the same scale parameter. But, at the same time, there were greater differences in the accuracy values. It was not only true in terms of the maximum value, although there were typically higher values up to the L5 level, but above this value the classification accuracies in the 10L version fell sharply compared to the 100L, where the decline was more gradual. Accordingly, we can conclude that the large difference between the same levels (L5) was caused by the built shapes of the individual segments. Segments of the region-growing algorithm depend on random seeds, which resulted in two different shapes. Although the construction of the 100L version is more time-consuming and the running time is slightly longer, the more detailed construction is worth it in terms of the results, as detailed analyses have not yet been exemplified in this field.

The results can affect forest management practices in order to improve the chance of identifying invasive tree species. The two invasive tree species selected have relevant differences in their environmental adaptation traits compared to other traditional temperate zone forest tree species: such as high growth and reproduction rates, and efficient dispersal accompanied with high tolerance to drought and air pollution (Cierjacks et al., 2013; Cronk & Fuller, 1995; Feret, 1985; Landenberger et al., 2009; Nava, 2014). In addition, the tree features of these two species are also different from the traditional forest tree species (e.g., Cierjacks et al., 2013; Feret, 1985; Nava, 2014). Under these conditions, our elaborated multiapproach method showed 4.6% better OA with a real benefit of a more accurate mapping of the invasive Ailanthus tree. This option supports a more efficient identification of this invasive species and may facilitate timely intervention to avoid its spread in areas of interest. With the support of aerial imaging, tree composition can be mapped with high accuracy and monitored easily, quickly

and more accurately in order to detect the changes of invasive tree species both spatially and temporally (da Silva et al., 2023; Dyrmann et al., 2021). This also provides a valuable practical option in the mapping of forest trees where there are stands mixed with invasive tree species.

General limitation of aerial tree mapping can be that, in closed stands, the trees need to reach at least the main canopy layer due to become detectable from the above. Therefore, the method may be less applicable in the first-line defence against new invaders but could rather help in tracking and controlling their further spread in the area of interest. Another, more specific limitation of this approach is the complexity of the steps, which requires several software. Classification can be automated even by means of R or Python language environments, but the MRS requires eCognition, a proprietary software in order to improve the approach provided in this study. Therefore, our plan is to test the post-classification with other segmentation techniques next and automatize each step creating a workflow. Tree species mapping is possible with satellite images, too, but it needs further investigations: high spatial resolution usually paired with lower number spectral bands, and hyperspectral images (e.g., EnMap, PRISMA, DESIS) has 30 m of spatial resolution, which can impede the identification of single trees in a dense stock. This automated approach may provide a possible direction of more accurate data collection for understanding the compositions of dominant and scattered invasive forest tree species in various forest types and may help in achieving more successful forest management practices.

Conclusion

Our aim was to test a TDA and a post-classification technique to gain a more accurate image classification method for hyperspectral image processing in the field of forest management. Ten tree species were mapped, but the main focus was on the invasive species, black locust and Ailanthus tree. We found that the TDA successfully improved the OAs from 81.64% to 82.46%. SVM outperformed the RF classifier regarding the maximum OAs; however, the difference was below 1%, and the RF responded more sensitively to the number of MCs (more variables yielded better OAs). Generally, the TDA did not prove to be efficient but, especially in the case of Ailanthus, a sparsely distributed aggressive invasive species, this method combined with post-classification increased both the PA and UA with 40%. The post-classification segmentation resulted in 3.75% better results OAs (86.24%) and eliminated the salt-and-pepper error. Thus, the additional steps in the image processing, that is, pre-treatment (TDA) and post-classification, improved the OA with 4.6%. But the real benefit was a more accurate mapping of the invasive Ailanthus tree (43% better results on class level) and the sporadically appearing black locust trees (due to its low fraction was justified only by visual validation). These results can help in preserving the natural tree species structure, and thus, nature conservation with a more efficient identification of invasive species, and can facilitate timely intervention to avoid their spread in the area of interest.

Though our new approach needs further investigations and testing on different study sites, it provided efficient output on class level with the combination of OBIA and DL techniques, and traditional machine learning classifications of woodlands.

Acknowledgements

The research was supported by the professional support of the Doctoral Student Scholarship Program of the Co-operative Doctoral Program of the Ministry of Innovation and Technology, the K138079, K138503, K131478 and the KKP144068 Nemzeti Kutatási Fejlesztési Hivatal projects.

References

Abadi, M., Agarwal, A., Barham, P., Brevdo, E., Chen, Z., Citro, C. et al. (2016) Tensorflow: large-scale machine learning on heterogeneous distributed systems. *arXiv* [preprint] arXiv:1603.04467.

Aguirre-Gutiérrez, J., Seijmonsbergen, A.C. & Duivenvoorden, J.F. (2012) Optimizing land cover classification accuracy for change detection, a combined pixel-based and object-based approach in a mountainous area in Mexico. *Applied Geography*, **34**, 29–37. Available from: https://doi.org/10.1016/j.apgeog.2011.10.010

Aksoy, S. & Akcay, H.G. (2005) Multi-resolution segmentation and shape analysis for remote sensing image classification. *Proceedings of 2nd International Conference on Recent Advances in Space Technologies 2005*. RAST 2005, Istanbul, Turkey. Available from: https://doi.org/10.1109/rast.2005.1512638

Alonzo, M., McFadden, J.P., Nowak, D.J. & Roberts, D.A. (2016) Mapping urban forest structure and function using hyperspectral imagery and lidar data. *Urban Forestry & Urban Greening*, **17**, 135–147. Available from: https://doi.org/10.1016/j.ufug.2016.04.003

Amini, S., Homayouni, S., Safari, A. & Darvishsefat, A.A. (2018) Object-based classification of hyperspectral data using Random Forest algorithm. *Geo-spatial Information Science*, **21**(2), 127–138. Available from: https://doi.org/10.1080/10095020.2017.1399674

Asner, G.P., Jones, M.O., Martin, R.E., Knapp, D.E. & Hughes, R.F. (2008) Remote sensing of native and invasive species in

Hawaiian forests. *Remote Sensing of Environment*, **112**(5), 1912–1926. Available from: https://doi.org/10.1016/j.rse.2007.02.043

Baron, J., Hill, D.J. & Elmiligi, H. (2018) Combining image processing and machine learning to identify invasive plants in high-resolution images. *International Journal of Remote Sensing*, **39**(15–16), 5099–5118. Available from: https://doi.org/10.1080/01431161.2017.1420940

Belgiu, M. & Dragut, L. (2016) Random forest in remote sensing: a review of applications and future directions. *ISPRS Journal of Photogrammetry and Remote Sensing*, **114**, 2431. Available from: https://doi.org/10.1016/j.isprsjprs.2016.01.011

Bhosale, N., Manza, R., Kale, K., Scholar, R. & Professor, A. (2014) Analysis of effect of Gaussian, salt and pepper noise removal from noisy remote sensing images. *Proceedings of the Second International Conference on ERCICA*, pp. 386–390. Elsevier Publications. Available from: http://rameshmanza.in/Publication/Narayan_Bhosle/Analysis%20of%20Effect%20of%20Gaussian.pdf [Accessed 10 October 2022].

Blackman, A. (2013) Evaluating forest conservation policies in developing countries using remote sensing data: an introduction and practical guide. *Forest Policy and Economics*, **34**, 1–16. Available from: https://doi.org/10.1016/j.forpol.2013.04.006

Borengasser, M., Hungate, W.S. & Watkins, R. (2007) *Hyperspectral remote sensing: principles and applications*. Boca Raton: CRC Press.

Brahma, B., Nath, A.J., Deb, C., Sileshi, G.W., Sahoo, U.K. & Das, A.K. (2021) A critical review of forest biomass estimation equations in India. *Trees, Forests and People*, **5**, 100098. Available from: https://doi.org/10.1016/j.tfp.2021.100098

Breiman, L. (1984) *Classification and regression trees*, 1st edition. New York: Routledge. Available from: https://doi.org/10.1201/9781315139470

Breiman, L. (2001) Random forests. *Machine Learning*, **45**(1), 5–32. Available from: https://doi.org/10.1023/a:1010933404324

Brovkina, O., Latypov, I. & Cienciala, E. (2015) Estimating average tree crown size using high-resolution airborne data. *Journal of Applied Remote Sensing*, **9**(1), 096053. Available from: https://doi.org/10.1117/1.jrs.9.096053

Burai, P., Beko, L., Lenart, C., Tomor, T. & Kovacs, Z. (2019) Individual tree species classification using airborne hyperspectral imagery and lidar data. *2019 10th Workshop on Hyperspectral Imaging and Signal Processing: Evolution in Remote Sensing (WHISPERS)*. Amsterdam, Netherlands. Available from: https://doi.org/10.1109/whispers.2019.8921016

Casagrande, G. (2018) Small drones and geographic observation. In: Casagrande, G., Sik, A. & Szabó, G. (Eds.) *Small flying drones*, pp. 1–12. Cham: Springer. Available from: https://doi.org/10.1007/978-3-319-66577-1_1

Cierjacks, A., Kowarik, I., Joshi, J., Hempel, S., Ristow, M., von der Lippe, M. et al. (2013) Biological flora of the British Isles: *Robinia pseudoacacia*. *Journal of Ecology*, **101**(6), 1623–1640. Available from: https://doi.org/10.1111/1365-2745.12162

Congalton, R.G. (1991) A review of assessing the accuracy of classifications of remotely sensed data. *Remote Sensing of Environment*, **37**(1), 35–46. Available from: https://doi.org/10.1016/0034-4257

Cortes, C. & Vapnik, V. (1995) Support-vector networks. *Machine Learning*, **20**, 273–297.

Cronk, Q.C.B. & Fuller, J.L. (1995) *Plant invaders: the threat to natural ecosystems*. London: UK; Chapman & Hall Ltd.

da Silva, S.D.P., Eugenio, F.C., Fantinel, R.A., de Paula Amaral, L., dos Santos, A.R., Mallmann, C.L. et al. (2023) Modeling and detection of invasive trees using UAV image and machine learning in a subtropical forest in Brazil. *Ecological Informatics*, **74**, 101989. Available from: https://doi.org/10.1016/j.ecoinf.2023.101989

Drăguţ, L., Tiede, D. & Levick, S.R. (2010) ESP: a tool to estimate scale parameter for multiresolution image segmentation of remotely sensed data. *International Journal of Geographical Information Science*, **24**(6), 859–871. Available from: https://doi.org/10.1080/13658810903174803

Dyderski, M.K. & Jagodziński, A.M. (2020) Impact of invasive tree species on natural regeneration species composition, diversity, and density. *Forests*, **11**(4), 456. Available from: https://doi.org/10.3390/f11040456

Dyderski, M.K. & Pawlik, Ł. (2020) Spatial distribution of tree species in mountain national parks depends on geomorphology and climate. *Forest Ecology and Management*, **474**, 118366. Available from: https://doi.org/10.1016/j.foreco.2020.118366

Dyrmann, M., Mortensen, A.K., Linneberg, L., Høye, T.T. & Bjerge, K. (2021) Camera assisted roadside monitoring for invasive alien plant species using deep learning. *Sensors*, **21**(18), 6126. Available from: https://doi.org/10.3390/s21186126

El-Hattab, M.M. (2016) Applying post classification change detection technique to monitor an Egyptian coastal zone (Abu Qir Bay). *The Egyptian Journal of Remote Sensing and Space Science*, **19**(1), 23–36. Available from: https://doi.org/10.1016/j.ejrs.2016.02.002

EnMAP-Box Developers. (2019) *EnMAP-Box 3 - a QGIS Plugin to process and visualize hyperspectral remote sensing data*. Available at: https://enmap-box.readthedocs.io [Accessed 10 October 2022].

Farmonov, N., Amankulova, K., Szatmári, J., Sharifi, A., Abbasi-Moghadam, D., Mirhoseini, N.S.M. et al. (2023) Crop type classification by DESIS hyperspectral imagery and machine learning algorithms. *IEEE Journal of Selected Topics*

in Applied Earth Observations and Remote Sensing, **16**, 1576–1588.

Feret, P.P. (1985) Ailanthus: variation, cultivation, and frustration. *Journal of Arboriculture*, **11**(12), 361–368.

Guanter, L., Kaufmann, H., Segl, K., Foerster, S., Rogass, C., Chabrillat, S. et al. (2015) The EnMAP spaceborne imaging spectroscopy mission for earth observation. *Remote Sensing*, **7**, 8830–8857. Available from: https://doi.org/10.3390/rs70708830

Hamada, Y., Stow, D.A., Coulter, L.L., Jafolla, J.C. & Hendricks, L.W. (2007) Detecting tamarisk species (*Tamarix* spp.) in riparian habitats of Southern California using high spatial resolution hyperspectral imagery. *Remote Sensing of Environment*, **109**(2), 237–248.

Hanover, J.W. & Mebrahtu, T. (1991) *Robinia pseudoacacia*: temperate legume tree with worldwide potential. NFT Highlights, No. 91-03. Available at: http://www.winrock.org/forestry/factpub/FACTSH/R_pseudoacacia.html [Accessed 10 October 2022].

Hastie, T., Tibshirani, R. & Friedman, J. (2009) *The elements of statistical learning: data mining, inference, and prediction*, 2nd edition. New York: Springer, p. 745. Available from: https://doi.org/10.1007/978-0-387-84858-7

Heisey, R.M. (1990) Evidence for allelopathy by tree-of-heaven (*Ailanthus altissima*). *Journal of Chemical Ecology*, **16**(6), 2039–2055. Available from: https://doi.org/10.1007/BF01020515

Hinton, G.E., Osindero, S. & Teh, Y.W. (2006) A fast learning algorithm for deep belief nets. *Neural Computation*, **18**(7), 1527–1554. Available from: https://doi.org/10.1162/neco.2006.18.7.1527

Karpouzli, E. & Malthus, T. (2003) The empirical line method for the atmospheric correction of IKONOS imagery. *International Journal of Remote Sensing*, **24**(5), 1143–1150. Available from: https://doi.org/10.1080/0143116021000026779

Ke, Y., Quackenbush, L.J. & Im, J. (2010) Synergistic use of QuickBird multispectral imagery and LIDAR data for object-based forest species classification. *Remote Sensing of Environment*, **114**(6), 1141–1154. Available from: https://doi.org/10.1016/j.rse.2010.01.002

Kevey, B. & Borhidi, A. (2005) The acidophilous forests of the Mecsek and their relationship with the Balkan-Pannonian acidophilous forests. *Acta Botanica Hungarica*, **47**(3–4), 273–368. Available from: https://doi.org/10.1556/abot.47.2005.3-4.5

Lake, T.A., Briscoe Runquist, R.D. & Moeller, D.A. (2022) Deep learning detects invasive plant species across complex landscapes using Worldview-2 and Planetscope satellite imagery. *Remote Sensing in Ecology and Conservation*, **8**(6), 875–889. Available from: https://doi.org/10.1002/rse2.288

Lampe, J., Wells, K., Kortgaard, S., Reynolds, C., Ogushi, F. & Allen, T. (2021). *Exelis Visual Information Solutions Software*. Boulder, Colorado, United States. Available at: https://www.datanyze.com/companies/exelis-visual-informationsolutions/507343120 [Accessed 10 October 2022].

Landenberger, R.E., Warner, T.A. & McGraw, J.B. (2009) Spatial patterns of female *Ailanthus altissima* across an urban-to-rural land use gradient. *Urban Ecosystem*, **12**, 437–448. Available from: https://doi.org/10.1007/s11252-009-0087

Likó, S.B., Bekő, L., Burai, P., Holb, I.J. & Szabó, S. (2022) Tree species composition mapping with dimension reduction and post-classification using very high-resolution hyperspectral imaging. *Scientific Reports*, **12**(1), 20919. Available from: https://doi.org/10.1038/s41598-022-25404-x

Lv, Z.Y., Li, G., Jin, Z., Benediktsson, J.A. & Foody, G.M. (2020) Iterative training sample expansion to increase and balance the accuracy of land classification from VHR imagery. *IEEE Transactions on Geoscience and Remote Sensing*, **59**(1), 15012. Available from: https://doi.org/10.1109/TGRS.2020.2996064

Ma, L., Liu, Y., Zhang, X., Ye, Y., Yin, G. & Johnson, B.A. (2019) Deep learning in remote sensing applications: a meta-analysis and review. *ISPRS Journal of Photogrammetry and Remote Sensing*, **152**, 166–177. Available from: https://doi.org/10.1016/j.isprsjprs.2019.04.015

Manandhar, R., Odeh, I.O. & Ancev, T. (2009) Improving the accuracy of land use and land cover classification of Landsat data using post-classification enhancement. *Remote Sensing*, **1**(3), 330–344. Available from: https://doi.org/10.3390/rs1030330

Maurya, P., Das, A.K. & Kumari, R. (2021) Managing the blue carbon ecosystem: a remote sensing and GIS approach. In: Pandey, P.C. & Sharma, L.K. (Eds.) *Advances in remote sensing for natural resource monitoring*, pp. 249–268. Medford, MA: John Wiley & Sons, Inc. Available from: https://doi.org/10.1002/9781119616016.ch13

Melgani, F. & Bruzzone, L. (2004) Classification of hyperspectral remote sensing images with support vector machines. *IEEE Transactions on Geoscience and Remote Sensing*, **42**(8), 1778–1790. Available from: https://doi.org/10.1109/TGRS.2004.831865

Merentitis, A., Debes, C. & Heremans, R. (2014) Ensemble learning in hyperspectral image classification: toward selecting a favorable bias-variance tradeoff. *IEEE Journal of Selected Topics in Applied Earth Observations and Remote Sensing*, **7**(4), 1089–1102. Available from: https://doi.org/10.1109/jstars.2013.2295513

Mi, C., Huettmann, F., Guo, Y., Han, X. & Wen, L. (2017) Why choose random forest to predict rare species distribution with few samples in large undersampled areas? Three Asian crane species models provide supporting evidence. *PeerJ*, **5**, e2849. Available from: https://doi.org/10.7717/peerj.2849

Müller, R., Avbelj, J., Carmona, E., Gerasch, B., Graham, L., Günther, B. et al. (2016) The new hyperspectral sensor DESIS on the multi-payload platform MUSES iInstalled on the ISS. *The International Archives of the Photogrammetry,*

Remote Sensing and Spatial Information Sciences, XLI-B1. XXIII ISPRS Congress, 12–19 July 2016, Prague, Czech Republic. pp. 461–467. Available from: https://doi.org/10.5194/isprsarchives-XLI-B1-461-2016

Murty, M.N. & Raghava, R. (Eds.) (2016) Chapter 5: Kernel-based SVM. In: *Support vector machines and perceptrons*, pp. 57–67. Cham, Switzerland: Springer. Available from: https://doi.org/10.1007/978-3-319-41063-0_5

Nagy, G., Lóczy, D., Czigány, S., Pirkhoffer, E., Fábián, S.Á. & Ferk, M. (2020) Soil moisture retention on slopes under different agricultural land uses in hilly regions of southern Transdanubia. *Hungarian Geographical Bulletin*, **69**(3), 263–280. Available from: https://doi.org/10.15201/hungeobull.69.3.3

Nasir, H., Iqbal, Z., Hiradate, S. & Fujii, Y. (2005) Allelopathic potential of *Robinia pseudo-acacia* L. *Journal of Chemical Ecology*, **31**, 2179–2192. Available from: https://doi.org/10.1007/s10886-005-6084-5

Nava, S.C. (2014) *Ailanthus altissima (tree-of-heaven)*. New York: CABI Compendium, CABI Digital Library. Available from: https://doi.org/10.1079/cabicompendium.3889

Pu, R. (2017) *Hyperspectral remote sensing: fundamentals and practices*. Boca Raton: CRC Press. Available from: https://doi.org/10.1201/9781315120607

Radtke, A., Ambraß, S., Zerbe, S., Tonon, G., Fontana, V. & Ammer, C. (2013) Traditional coppice forest management drives the invasion of *Ailanthus altissima* and *Robinia pseudoacacia* into deciduous forests. *Forest Ecology and Management*, **291**, 308–317. Available from: https://doi.org/10.1016/j.foreco.2012.11.022

Rebbeck, J., Kloss, A., Bowden, M., Coon, C., Hutchinson, T.F., Iverson, L. et al. (2015) Aerial detection of seed-bearing female *Ailanthus altissima*: a cost-effective method to map an invasive tree in forested landscapes. *Forest Science*, **61**(6), 1068–1078. Available from: https://doi.org/10.5849/forsci.14-223

Richter, R., Reu, B., Wirth, C., Doktor, D. & Vohland, M. (2016) The use of airborne hyperspectral data for tree species classification in a species-rich central European forest area. *International Journal of Applied Earth Observation and Geoinformation*, **52**, 464–474. Available from: https://doi.org/10.1016/j.jag.2016.07.018

Shah, B. (1997) The checkered career of *Ailanthus altissima*. *Arnoldia (Boston)*, **57**(3), 21–27.

Shiferaw, H., Bewket, W. & Eckert, S. (2019) Performances of machine learning algorithms for mapping fractional cover of an invasive plant species in a dryland ecosystem. *Ecology and Evolution*, **9**(5), 2562–2574. Available from: https://doi.org/10.1002/ece3.4919

Shorten, C. & Khoshgoftaar, T.M. (2019) A survey on image data augmentation for deep learning. *Journal of Big Data*, **6**, 1–48. Available from: https://doi.org/10.1186/s40537-019-0197-0

Stuffler, T., Kaufmann, C., Hofer, S., Förster, K.P., Schreier, G., Mueller, E.A. et al. (2007) The EnMAP hyperspectral imager—an advanced optical payload for future applications in earth observation programmes. *Acta Astronautica*, **61**(1–6), 115–120. Available from: https://doi.org/10.1016/j.actaastro.2007.01.033

Szabó, L., Abriha, D., Phinzi, K. & Szabó, S. (2021) Urban vegetation classification with high-resolution PlanetScope and SkySat multispectral imagery. *Landscape & Environment*, **15**(1), 66–75. Available from: https://doi.org/10.21120/LE/15/1/9

Tarantino, C., Casella, F., Adamo, M., Lucas, R., Beierkuhnlein, C. & Blonda, P. (2019) *Ailanthus altissima* mapping from multi-temporal very high resolution satellite images. *ISPRS Journal of Photogrammetry and Remote Sensing*, **147**, 90–103. Available from: https://doi.org/10.1016/j.isprsjprs.2018.11.013

Thakkar, A.K., Desai, V.R., Patel, A. & Potdar, M.B. (2017) Post-classification corrections in improving the classification of land use/land cover of arid region using RS and GIS: the case of Arjuni watershed, Gujarat, India. *The Egyptian Journal of Remote Sensing and Space Science*, **20**(1), 79–89. Available from: https://doi.org/10.1016/j.ejrs.2016.11.006

Tharwat, A. (2021) Classification assessment methods. *Applied Computing and Informatics*, **17**(1), 168–192. Available from: https://doi.org/10.1016/j.aci.2018.08.003

Vangi, E., D'Amico, G., Francini, S., Giannetti, F., Lasserre, B., Marchetti, M. et al. (2021) The new hyperspectral satellite PRISMA: imagery for forest types discrimination. *Sensors*, **21**(4), 1182. Available from: https://doi.org/10.3390/s21041182

Vo, Q.T., Oppelt, N., Leinenkugel, P. & Kuenzer, C. (2013) Remote sensing in mapping mangrove ecosystems - an object-based approach. *Remote Sensing*, **5**(1), 183–201. Available from: https://doi.org/10.3390/rs5010183

Vorster, A.G., Evangelista, P.H., Stovall, A.E. & Ex, S. (2020) Variability and uncertainty in forest biomass estimates from the tree to landscape scale: the role of allometric equations. *Carbon Balance and Management*, **15**, 1–20. Available from: https://doi.org/10.1186/s13021-020-00143-6

Wang, A., Wang, Y. & Chen, Y. (2019) Hyperspectral image classification based on convolutional neural network and random forest. *Remote Sensing Letters*, **10**(11), 1086–1094. Available from: https://doi.org/10.1080/2150704X.2019.1649736

Wilfong, B.N., Gorchov, D.L. & Henry, M.C. (2009) Detecting an invasive shrub in deciduous forest understories using remote sensing. *Weed Science*, **57**(5), 512–520. Available from: https://doi.org/10.1614/WS-09-012.1

Zhang, C., Atkinson, P.M., George, C., Wen, Z., Diazgranados, M. & Gerard, F. (2020) Identifying and mapping individual plants in a highly diverse high-elevation ecosystem using UAV imagery and deep learning. *ISPRS Journal of Photogrammetry and Remote Sensing*, **169**, 280–291.

Zhang, C. & Xie, Z. (2012) Combining object-based texture measures with a neural network for vegetation mapping in the Everglades from hyperspectral imagery. *Remote Sensing of Environment*, **124**, 310–320. Available from: https://doi.org/10.1016/j.rse.2012.05.015

Zhang, Y. & Shao, Z. (2021) Assessing of urban vegetation biomass in combination with LiDAR and high-resolution remote sensing images. *International Journal of Remote Sensing*, **42**(3), 964–985. Available from: https://doi.org/10.1080/01431161.2020.1820618

Zhao, D., Pang, Y., Liu, L. & Li, Z. (2020) Individual tree classification using airborne LiDAR and hyperspectral data in a natural mixed forest of northeast China. *Forests*, **11**(3), 303. Available from: https://doi.org/10.3390/f11030303

Zhao, W. & Du, S. (2016) Learning multiscale and deep representations for classifying remotely sensed imagery. *ISPRS Journal of Photogrammetry and Remote Sensing*, **113**, 155–165. Available from: https://doi.org/10.1016/j.isprsjprs.2016.01.004

Zhou, S., Xue, Z. & Du, P. (2019) Semisupervised stacked autoencoder with cotraining for hyperspectral image classification. *IEEE Transactions on Geoscience and Remote Sensing*, **57**(6), 3813–3826. Available from: https://doi.org/10.1109/TGRS.2018.2888485

Zhu, X.X., Tuia, D., Mou, L., Xia, G.S., Zhang, L., Xu, F. et al. (2017) Deep learning in remote sensing: a comprehensive review and list of resources. *IEEE Geoscience and Remote Sensing Magazine*, **5**(4), 8–36. Available from: https://doi.org/10.1109/MGRS.2017.2762307

